Unidirectional recruitment relations between proteins can be determined by a CRISPR/dCas9 recruitment assay

Ido Lavi[#], Supriya Bhattacharya[#], Ola Orgil, Nir Avital, Guy Journo, Vyacheslav Gurevich and Meir Shamay*

Daniella Lee Casper Laboratory in Viral Oncology, Azrieli Faculty of Medicine, Bar-Ilan University, Safed, Israel 1311502

[#] These authors contributed equally to this work

* Corresponding author

Meir Shamay

Email: meir.shamay@biu.ac.il

Running Title: CRISPR/dCas9 recruitment assay

Author Contributions: Conceived and designed the experiments: I.L., S.B., M.S. Performed the experiments: I.L., S.B., Analyzed the data: I.L., S.B., G.J. & M.S. Generated tools & reagents: O.O., N.A., V.G., S.B., Wrote the paper: M.S.

Competing Interest Statement: The authors declare no competing financial interests.

Keywords: CRISPR/Cas9, dCas9, KSHV, HHV-8, LANA, MeCP2, Recruitment.

Abstract

Directional recruitment of protein complexes is critical for proper function of many nuclear processes. Here we present CRISPR-PITA (**P**rotein **I**nteraction and **T**elomere Recruitment **A**ssay), an assay that determines the ability of a given protein to recruit any other nuclear factor. The protein of interest is directed via CRISPR/dCas9, a dead Cas9 that does not cut DNA, to a repeat sequence, such as telomeres, to obtain dots that are easily detectable by microscopy. The recruitment of endogenous nuclear proteins to these dots can then be visualized using specific antibodies. We determined recruitment abilities in CRISPR-PITA to methyl-CpG binding protein MeCP2, histone deacetylase 1 (HDAC1), heterochromatin protein 1 (HP1α), and the latency-associated nuclear antigen (LANA) encoded by Kaposi's sarcoma associated herpesvirus (KSHV, HHV-8). LANA was able to recruit its known interactors ORC2 and SIN3A to LANA-telomere dots. In contrast, LANA was unable to recruit MeCP2 whereas MeCP2 was able to recruit LANA. Similarly, HDAC1 that interacts with MeCP2 through the transcriptional-repression domain (TRD) same as LANA, was unable to recruit MeCP2, but MeCP2 recruited HDAC1. One important function of LANA is to tether the viral episomal genomes to the cellular chromosomes during cell division. The unidirectional recruitment of LANA by MeCP2, makes MeCP2 a candidate anchor for KSHV genome tethering by LANA. We found that cells derived from Rett syndrome and express a mutant MeCP2 (T158M), impaired in DNA binding, cannot support KSHV genome maintenance. In summary, we describe a broadly applicable protein recruitment assay based on CRISPR/dCas9.

Significance Statement

CRISPR/Cas9 is a revolutionary system that has profoundly impacted biology research. Here we present another application for CRISPR/Cas9, in evaluating recruitment relations between nuclear proteins. A protein of interest is directed to a repeat sequence via the catalytically inactive Cas9 (dCas9) to generate easily detectable dots. Then, the recruitment of other nuclear proteins to these dots can be evaluated. Using this assay, we show that some interacting proteins have a unidirectional recruitment property, where only one of the proteins can recruit its partner. We propose that available interacting domains can force this unidirectional recruitment. Using this recruitment assay, we found unidirectional recruitment of the KSHV encoded LANA and HDAC1 by MeCP2. Furthermore, this unidirectional recruitment is critical for viral latency, since LANA fails to maintain the viral genomes in MeCP2 mutant cells.

Main Text

Introduction

For many nuclear processes directional recruitment of protein complexes is critical for proper function. Transcription factor that binds a specific DNA sequence recruits co-activators and general transcription factors that results in subsequent recruitment of RNA polymerase leading to gene expression. In this scenario, it is expected that a transcription factor of interest will recruit the co-activator. However, the co-activator that is recruited by other transcription factors as well, should not recruit the transcription factor of interest. One example of recruitment directionality is the estrogen receptor, where the combination of ligand binding, dimerization and sequence specific DNA binding are required to generate high affinity surface to recruit co-activator proteins (1). This conformational change upon DNA binding and dimerization will favor binding and recruitment of co-activator to enhancer/promoter bound receptor and minimize interaction with DNA-free receptor. Another example is the enhanceosome, where coordinated activation of three distinct transcription factors and the architectural protein HMG I(Y) bind cooperatively to interferon-beta enhancer (2). Together they form high affinity surface to efficiently recruit the co-activator CBP (3). Therefore, an assay that can determine recruitment relations between interacting proteins may provide deeper understanding of biological systems. Although Chromatin immunoprecipitation (ChIP) assays may assist in this regard, there is a lack of an easy recruitment assay.

MeCP2 binds methylated DNA and recruits co-repressor complexes to execute the readout of CpG methylation into transcription repression (4). Several studies detected interaction between MeCP2 and histone deacetylase 1 (HDAC1), and recruitment of histone deacetylase activity is important for transcription repression imposed by MeCP2 (5, 6). MeCP2 and HDAC1 represent an example of two proteins that interact in the nucleus. While MeCP2 recruits HDAC1 to methylated regions in order to repress transcription, we expect that HDAC1 should not recruit MeCP2 to promoters in those cases where HDAC1 is recruited by other transcription factors. Another protein that plays important role in transcription repression is heterochromatin protein 1 (HP1). HP1 interacts with the repressive mark histone 3 lysine 9 tri-methylation (H3K9Me3) and via recruitment of SUV39H1, the histone H3K9Me3 methyltransferase, leads to spreading of this heterochromatin repressive histone mark (7, 8). HP1 has been shown to interact with MeCP2 (9, 10), but whether HP1 can recruit MeCP2 is an open question.

Kaposi's sarcoma associated herpesvirus (KSHV, HHV-8) is associated with several human malignancies (11, 12). Like all herpes viruses KSHV has two phases: latent (dormant) and lytic (productive) cycle. During latency the viral genomes reside in the nucleus of infected cells as large non-integrated plasmids, known as

viral episomes. All KSHV infected cells express LANA, and LANA is essential for viral latency (13-15). LANA binding to the viral episomes is critical both for replication by recruitment of the cellular replication machinery to the viral genomes (16, 17), and for maintenance by tethering the viral episomes to the cell chromosomes during cell division (18, 19). Multiple LANA binding sites (LBS1 and LBS2) (20, 21) within the KSHV terminal repeats, and its oligomerization ability (22, 23) create clearly visible LANA dots in KSHV-infected cells. In contrast, LANA is equally distributed in the nucleus when it is expressed in un-infected cells. So, it is challenging to determine whether LANA or the viral genomes are the recruiters of cellular factors.

Cas9 is an endonuclease that can be directed to different DNA targets that are complimentary to a guide RNA and contain a PAM sequence (24). Soon after the discovery of this property, many applications of this sequence specific targeting of Cas9 emerged. For targeting purposes, the endonuclease is no longer needed, and a catalytically dead mutant Cas9 (dCas9) that still retains DNA binding capability was created (24, 25). Targeting this dCas9 to promoter sequences results in transcription activation or repression depending on the fused domains and the targeting location relative to the transcription start site (25, 26). Shortly after the creation of the dCas9 it was directed to repeat elements for the visualization of these elements in fixed (27) and live cells (28, 29). Targeting dCas9 to telomeres was also applied in an in-vivo mouse model (30).

Here we present a simple recruitment assay based on CRISPR/Cas9. We combined the ability of the SunTag system (31) to gather up to ten molecules of a protein of interest with CRISPR/dCas9 targeted to a repeat sequence such as telomeres. The ability of this protein to recruit endogenous or fluorescently tagged proteins to these telomere dots is determined. Interestingly, we find that the recruitment does not always work bi-directionally. LANA fails to recruit MeCP2, but MeCP2 efficiently recruits LANA. The unidirectional recruitment of LANA by MeCP2 raised the possibility that MeCP2 may serve as a protein anchor for LANA tethering. Indeed, we found that the virus fails to maintain its episomes in cells expressing a mutant MeCP2. We also investigated the recruitment relations between MeCP2 and HDAC1, and found that MeCP2 can recruit HDAC1, but HDAC1 is unable to recruit MeCP2. While both LANA and HDAC1 interact with the transcriptional-repression domain (TRD) of MeCP2, heterochromatin protein 1 (HP1α) interacts the N-terminal domain (amino acids 1–55) of MeCP2 (9). Interestingly, we found that HP1α is able to recruit MeCP2. In summary, CRISPR-PITA can determine recruitment relations between proteins and highlight the critical role of available interaction domains to determine recruitment directionality.

Results

Creation of visible dots at the telomeres with dCas9-SunTag and Fc-LANA

The ability of dCas9 to direct proteins of interest to any genomic locus makes it an ideal system for a recruitment assay. Previous studies used the dCas9 system for labeling locus specific regions and targeting dCas9 to repeat genomic regions generated visible dots in fixed and live cells (27-29). In order to enhance dot formation, we utilized the SunTag system where tandem epitopes can concentrate multiple molecules of an antibody-fused protein that recognizes this epitope (up-to 10 with the tag used in this study) (31). In our case the tandem epitopes are fused to dCas9 and the antibody Fc is fused to our protein of interest (**Fig. 1A**).

For a proof of concept, we used KSHV encoded LANA that localizes in large dots together with the viral episomes in KSHV infected cells but is equally distributed in the nucleus when expressed in un-infected cells (32). Transfection of LANA fused with the antibody Fc (Fc-LANA) together with dCas9 and sgRNA for telomere repeat sequence, resulted in LANA-telomere-dots that were visible by immuno-fluorescent assay (IFA) for LANA (**Fig. 1B**). When the dCas9 was omitted from the mix LANA could not generate nuclear dots, suggesting that LANA-telomere-dots are dependent on the targeting of LANA to telomeres via dCas9. To validate that LANA was targeted to the telomeres we used an antibody against the telomeric repeat factor 2 (TRF2), and indeed Fc-LANA co-localized with TRF2 when co-transfected with dCas9 and sgTelomere (**Fig. S1A**). The larger dots of TRF2 observed in cells where LANA is targeted to telomeres via dCas9-SunTag, can be explained by LANA's ability to oligomerize and cluster several viral genomes (20, 22, 23, 33-35). Studies of the LANA oligomerization property identified a LANA oligomerization mutant (22, 23). Therefore, we created this LANA oligomerization mutant (F1037A/F1041A) in the context of Fc-LANA (Fc-LANA-mutant) and compared the dot size to Fc-LANA. As expected, the LANA oligomerization mutant created smaller telomere dots compared to wt LANA (**Fig. S1B**), indicating that targeting to telomeres can also determine oligomerization ability and identify oligomerization mutants. Altogether, these experiments indicate that we can generate LANA dots in un-infected cells using the dCas9 SunTag system.

LANA recruits ORC2 and SIN3A but not MeCP2

In this assay a protein of interest is targeted to telomeres via dCas9, and the recruitment of endogenous proteins to these dots is detected by immunofluorescence assay (**Fig. 1C**). We termed this method CRISPR-PITA for Protein Interaction and Telomere recruitment Assay. We performed the CRISPR-PITA assay for ORC2, a subunit of the Origin Replication Complex (ORC), previously reported to interact with LANA

146 and localize with LANA-episome-dots (23, 36-38). ORC2 was recruited by LANA, as was determined by
147 the easily detected dots that co-localized with LANA-telomere-dots (**Fig. 2A**). It is important to note, that
148 while the dCas9 and Fc-LANA were ectopically expressed, the recruited proteins are endogenous proteins,
149 indicating the ability of LANA to recruit the endogenous ORC2. To quantify recruitment in unbiased
150 manner, we created a measurement tool for dot formation. Using ImageJ the number of large dots and small
151 dots of the analyzed protein in each cell are counted and then the ratio between large and small dots for
152 each cell is calculated. The average of the ratios measured in several individual cells (n=15) is presented.
153 This measurement (average [large/small dots]) clearly shows that ORC2 was recruited to LANA-telomere-
154 dots.

155 Several studies reported on interaction between LANA and the corepressor protein SIN3A (mSin3a) (38,
156 39), and the methyl-CpG binding protein MeCP2 (40-42), but it was reported that MeCP2 is not associated
157 with LANA dots in KSHV infected cells (43). We found that Fc-LANA recruited SIN3A to LANA-
158 telomere-dots, both by visual observation and by our quantification (average [large/small dots]) (**Fig. 2B**).
159 Analysis of MeCP2 recruitment via the CRISPR-PITA revealed no recruitment of MeCP2 to LANA-
160 telomere-dots (**Fig. 2C**). Co-immunoprecipitation assay indicated that Fc-LANA was able to
161 immunoprecipitate MeCP2 (**Fig. S2**), excluding the possibility that the lack of recruitment is due to the
162 fusion between Fc and LANA that disrupted the interaction between LANA and MeCP2. Another
163 possibility to explain the lack of MeCP2 recruitment by LANA, is that as a methylated DNA binding
164 protein, it is engaged in binding methylated DNA and therefore not available to be recruited to LANA-
165 telomere-dots. To test this, we performed the CRISPR-PITA in cells with knock-out (KO) of DNMT1 and
166 DNMT3b (HCT DKO) that were reported to lose over 95% of their CpG methylation (44). Even in HCT
167 DKO, Fc-LANA could not recruit MeCP2 to LANA-telomere-dots (**Fig. S3**), suggesting that protein
168 availability could not explain the lack of recruitment in this case. Immunofluorescence assays for ORC2,
169 SIN3A and MeCP2 in KSHV-infected PEL (BCBL1) cells, revealed that while ORC2 and SIN3A were
170 found associated with LANA-episome-dots, MeCP2 was not associated with the LANA-episome-dots (**Fig.
171 S4**), supporting the ability of the CRISPR-PITA to predict recruitment ability between proteins.

172 **MeCP2 recruits LANA**

173 The observation that Fc-LANA could not recruit MeCP2, despite their documented interaction (40-42) and
174 co-immunoprecipitation performed in this study (**Fig. S2**), highlights the importance to determine
175 recruitment relations between proteins. Krithivas et al. have shown that expression of human MeCP2 is
176 able to recruit LANA to heterochromatin in NIH 3T3 mouse cells (40). Therefore, we tested the ability of

177 Fc-MeCP2 to recruit LANA to MeCP2-telomere-dots. Cells were co-transfected with dCas9, sgTelomere,
178 Fc-MeCP2 and expression vectors for GFP-LANA or GFP alone as control. Fc-MeCP2 was able to recruit
179 GFP-LANA to MeCP2-telomere-dots, but not GFP alone, supporting the ability of MeCP2 to recruit LANA
180 (**Fig. 3A**). LANA contains three distinct domains, the N-terminal region (AA 1-329), the C-terminal (AA
181 936-1162), and a middle repeat region. Both the N and C-terminal regions have been shown to mediate
182 chromosome association; the N via binding to core histones H2A and H2B (45), while for the C-terminal
183 several candidates were identified including MeCP2, DEK and RING3 (40, 41, 46). To determine the region
184 of LANA sufficient for recruitment by MeCP2, we performed CRISPR-PITA by Fc-MeCP2 for LANA
185 N+C, LANA N and LANA C. While both LANA N+C and LANA C were efficiently recruited by MeCP2,
186 no recruitment was observed with the N-terminal (**Fig. 3B**). This result is in agreement with a previous
187 study that located the interaction between LANA and MeCP2 to the C-terminal region (41). This result
188 indicates that despite the high concentration of the recruiter protein at telomeres, still CRISPR-PITA
189 requires specific interaction, as both the N-terminal of LANA and GFP-alone were not recruited by MeCP2
190 in our assay. This set of experiments highlights the distinction between interaction and recruitment, while
191 LANA and MeCP2 were shown to interact with each other, still MeCP2 can recruit LANA, but LANA
192 cannot recruit MeCP2.

193 **MeCP2 is able to recruit HDAC1, but HDAC1 is unable to recruit MeCP2**

194 Several studies detected interaction between MeCP2 and histone deacetylase 1 (HDAC1), and this
195 recruitment of histone deacetylase activity is important for transcription repression imposed by MeCP2 (5,
196 6). MeCP2 and HDAC1 represent an example where two proteins can interact to form protein complexes
197 in the nucleus. We expect that MeCP2 should recruit HDAC1 to methylated regions in order to repress
198 transcription, but HDAC1 should not recruit MeCP2 to the promoters where it is recruited by other
199 transcription factors. Therefore, we applied the CRISPR-PITA to determine recruitment relations between
200 these two cellular proteins. CRISPR-PITA revealed that Fc-MeCP2 efficiently recruits HDAC1 to MeCP2-
201 telomere-dots (**Fig. 4A**). In contrast, Fc-HDAC1 failed to recruit MeCP2 to HDAC1-telomere-dots both in
202 HCT (**Fig. 4B**) and HCT DKO cells (**Fig. 4C**). Thus, in the context of MeCP2 and HDAC1, recruitment is
203 also unidirectional, enabling MeCP2 to recruit HDAC1 to repress transcription, but preventing the
204 mislocalization of MeCP2 by HDAC1.

205 **Heterochromatin protein 1 is able to recruit MeCP2**

206 Both LANA and HDAC1 interact with the same region of MeCP2, the transcriptional-repression domain
207 (TRD), that is located next to the methyl-CpG-binding domain (MBD) (35, 40). In contrast,

208 Heterochromatin protein 1 (HP1α) interacts with the N-terminal domain (amino acids 1–55) of MeCP2 (9).
209 We hypothesized that since HP1α interacts with a different domain that might be available for interaction
210 also in its DNA-free state, HP1α might be able to recruit MeCP2. Interestingly, in CRISPR-PITA we found
211 that Fc-HP1α was able to recruit MeCP2 (**Fig. 5**). This result supports the notion that available interacting
212 domains determine recruitment directionality.

213 **Rett syndrome mutant MecP2 cannot support KSHV maintenance during latency**

214 One important function of LANA is to maintain the viral episomal genomes, by tethering the viral genomes
215 to cellular chromosomes during cell division, ensuring they remain in the nucleus once nuclear envelope is
216 reformed. To do so, LANA directly binds the LANA binding sites (LBS1 and LBS2) (20, 21) on the viral
217 genomes, and associates with cellular chromosomes. Our finding that MeCP2 recruits LANA, but LANA
218 cannot recruit MeCP2, suggests that the interaction with MeCP2 is permitted only once it is bound to
219 methylated DNA, and therefore may be a potential candidate for LANA tethering. Sporadic mutations in
220 MeCP2 are associated with most cases of Rett syndrome (RTT), a severe X-linked neurodevelopmental
221 disorder in humans. (47). Lymphoblastoid Cell Lines (LCLs) derived from RTT patients expressing wild-
222 type (wt) MeCP2 allele, mutant T158M (that cannot bind methylated DNA), and 803delG (deletion of the
223 C' terminus) of MeCP2 (48) were tested for their ability to support KSHV episome maintenance. Cells
224 were infected with rKSHV (rKSHV.219) expressing GFP and maintenance of the viral episomal DNA and
225 the percentages of GFP positive cells were analyzed (**Fig. 6 A & B**). While both wt and 803delG efficiently
226 supported viral latency, the MeCP2 mutant in the MBD that cannot bind DNA (T158M) could not. This
227 result indicates that a functional MeCP2 that is able to bind methylated DNA is essential for KSHV genome
228 maintenance. LANA has been shown to bind both the MBD and TRD of MeCP2 (41). To determine if
229 LANA can be recruited by the T158M mutant, we cloned it into Fc-MeCP2 and performed CRISPR-PITA
230 assay. We found that MeCP2 T158M mutant can recruit LANA (although to a lesser extent), when it is
231 artificially targeted to chromatin by dCas9 (**Fig. 6C**). MBD deletion mutant, partially lost the ability to
232 recruit LANA when artificially targeted to chromatin. To assay for both abilities to bind LANA and to bind
233 methylated DNA, we harnessed a specific feature of MeCP2 to localize to heterochromatin loci in mouse
234 cells. This assay is typically performed in NIH 3T3 cells, since they express very low levels of endogenous
235 MeCP2 (40, 49). Similar to previous studies (40, 41), we found that LANA can be efficiently recruited to
236 heterochromatin when co-transfected with MeCP2 (**Fig. 6D**). In contrast, both T158M and MBD-del
237 mutants were not associated with heterochromatin, and therefore could not recruit LANA to
238 heterochromatin loci. Altogether, we found that Rett syndrome mutant MeCP2 T158M, that cannot recruit

239 LANA to methylated DNA, also cannot support KSHV episome maintenance. We revealed a critical role
240 for MeCP2 in KSHV episome maintenance by LANA.

241 **Discussion**
242
243 A powerful method to study recruitment is the Chromatin immunoprecipitation (ChIP) assay, that can detect
244 association of proteins with specific DNA sequences (50, 51). ChIP assays require fixation, proper shearing
245 of the chromatin, and special antibodies that can perform the immunoprecipitation of the cross-linked
246 chromatin. In many cases even when two or more proteins are associated with the same genomic region, it
247 is hard to evaluate the relationship between the proteins and determine essential factors for the recruitment.
248 Although this limitation can be overcome by using Knockout (KO) or Knockdown (KD) of one protein and
249 testing the ability of other proteins to be recruited to DNA/chromatin in the absence of that protein, this
250 raises additional challenges in creating KO or KD of the target gene. The SOS-recruitment assay (SRA)
251 can identify protein-protein interactions via recruitment of a "prey" protein by a membrane associated
252 "bait" (52). This is a powerful method to identify protein-protein interactions, but the limitation of this
253 method is that both the "prey" and the "bait" are ectopically expressed, and interaction takes place in the
254 cytoplasm of yeast cells, which is less relevant for protein complexes in the nucleus. These assays most
255 often express a random library with partial protein sequences, and therefore cannot predict the ability to
256 recruit the full-length protein with its multiple protein-protein, protein-RNA or protein-DNA interactions
257 that might alter its ability to be recruited. Another recruitment assay is based on integration of the *lac*O
258 array into the genome and directing the protein of interest to this array via fusion to the Lac-repressor (53,
259 54). One limitation of this assay is the limited number of cell lines that were generated to contain integration
260 of this *lac*O array.

261 Here we describe a simple method to test for recruitment relations between proteins. This method does not
262 require chromatin shearing and can be performed with various antibodies that can recognize the native form
263 of proteins, and in the absence of such an antibody a recruitment of fluorescently labeled proteins can be
264 observed. To obtain visible dots we combined the ability of the repeated epitope SunTag with dCas9
265 targeted to a repetitive genomic sequence such as the telomeres. Although targeting dCas9 to telomeres has
266 been performed previously to follow nuclear events such as, liquid–liquid phase separation (LLPS), or the
267 generation of heterochromatin (55, 56), but has not been applied to test recruitment directionality. Using
268 this method we found unidirectional recruitment relations between proteins. Our results with CRISPR-
269 PITA, indicated that LANA was able to recruit ORC2 and SIN3A, but was unable to recruit MeCP2 to
270 LANA-telomere-dots. While it has been shown that ORC2 localizes with LANA dots (23, 36-38), and
271 MeCP2 does not (43), there was no published data on SIN3A localization in KSHV infected cells. So, we

272 performed immunofluorescence assay in KSHV-infected BCBL1 cells and found that both ORC2 and
273 SIN3A were associated with LANA dots, but MeCP2 was not. These results are in agreement with CRISPR-
274 PITA, supporting the ability of CRISPR-PITA to predict recruitment ability of proteins. The recruitment
275 of GFP-LANA by Fc-MeCP2 also suggests that CRISPR-PITA can be done without cell fixation or
276 immunofluorescence, but directly via detection of fluorescently-labeled proteins. This property might be
277 more relevant in cases where CRISPR-PITA is applied for screening purposes.

278 The combination of both the SunTag and a repeat element in targeting the protein of interest, results in high
279 protein concentration at specific nuclear locations. One concern that might be raised is whether the
280 recruitment we observed with CRISPR-PITA is specific or an artifact of the high protein concentration. To
281 test this possibility, we performed the CRISPR-PITA with Fc-MeCP2 and LANA deletion mutants. We
282 found that Fc-MeCP2 recruited the C-terminal of LANA, but not its N-terminal. Interaction of LANA C-
283 terminal domain with MeCP2 is in agreement with a previous study for LANA (41). The related gamma-
284 2 herpesvirus, herpesvirus saimiri (HVS) encodes for ORF73, a functional homolog of KSHV encoded
285 LANA (also known as ORF73). Also HVS encoded ORF73 interacts with MeCP2 via its C-terminal domain
286 (49). The lack of recruitment for the N-terminal domain of LANA, indicated that recruitment is still specific
287 and requires the interaction domain. Another support for the specific recruitment by CRISPR-PITA is the
288 lack of recruitment observed for GFP alone. A growing list of nuclear proteins with intrinsically disordered
289 regions and RNA/DNA binding properties can promote liquid–liquid phase separation (LLPS); both LANA
290 and MeCP2 possess this property (57, 58). Rett syndrome MeCP2 mutants, including T158M, are impaired
291 in LLPS formation. Since T158M mutant still can recruit LANA in CRISPR-PITA, indicates that the
292 recruitment we observed is not dependent on LLPS formation.

293 The inability of LANA to recruit MeCP2, despite their documented interaction prompted us to test whether
294 MeCP2 can recruit LANA. Indeed, in CRISPR-PITA Fc-MeCP2 was able to recruit LANA. This result
295 comes in agreement with a previous study where MeCP2 recruited LANA to mouse heterochromatin
296 structures (40). This result also highlights the importance of a recruitment assay as recruitment is not
297 always bi-directional, and in many cases should be functionally unidirectional. One of LANA functions
298 where unidirectional recruitment seems essential, is LANA tethering of the viral episomal genome to the
299 cell chromosomes during cell division. Therefore, we tested the possible role of MeCP2 in KSHV episome
300 maintenance. We found that Rett syndrome mutant MeCP2, that cannot bind methylated DNA (T158M),
301 could not support KSHV latency. Our result suggests that in addition to LANA interaction with histones
302 (45), MeCP2 adds another layer to secure chromosome tethering (suggested model in **Fig. 7**). Similar to
303 KSHV encoded LANA, HVS encoded ORF73 has a critical role in viral episomal genome maintenance

304 (59). MeCP2 has been shown to be essential for tethering of the viral genomes by ORF73 to maintain
305 HVS latency (49). Therefore, our observation that MeCP2 is essential for episome maintenance, seems to
306 be conserved between KSHV and HVS. In this scenario LANA/ORF73 binds MeCP2 to anchor the viral
307 episomes to cellular chromosomes. If the anchor (MeCP2) is free (not bound to DNA/chromosome), this
308 may lead to viral loss. Therefore, in this case unidirectional recruitment is a matter of survival or extinction.

309 A nice example of directional recruitment is the case of MeCP2 that binds methylated DNA and recruits
310 co-repressor complexes including HDAC1 (5, 6). In this case we expect that MeCP2 should recruit HDAC1,
311 leading to transcription repression. On the other hand, HDAC1 is recruited by many transcription factors
312 to generate repressive chromatin. Therefore, we expect that it should not recruit MeCP2 to all the
313 chromosome locations it is recruited by other transcription repressors. Indeed, we found that Fc-MeCP2
314 was able to recruit HDAC1 to MeCP2-telomere-dots, but Fc-HDAC1 was unable to recruit MeCP2. How
315 come two proteins that interact with each other can generate unidirectional recruitment? MeCP2 is an
316 intrinsically disordered protein that is monomeric in solution even at high concentrations but dimerizes
317 upon DNA binding (60, 61). Both LANA and HDAC1 interact with the transcriptional-repression domain
318 (TRD) of MeCP2 (6, 41) that is located next to the methyl-CpG-binding domain (MBD). In contrast, HP1α
319 interacts with the N-terminal domain (amino acids 1–55) of MeCP2 (9). Therefore, while the TRD domain
320 should be available for interaction only upon DNA binding and MeCP2 dimerization, we predicted that the
321 N-terminal domain might be available for interaction also in the form of DNA-free MeCP2. Indeed, we
322 found that HP1α is able to recruit MeCP2 to HP1α-telomere-dots. Based on these characteristics and our
323 CRISPR-PITA results we came to the following model; when MeCP2 is not associated with DNA it is a
324 monomer and therefore the TRD is not available to interact and therefore cannot be recruited by HDAC1
325 and LANA. When MeCP2 binds methylated DNA its conformation changes so the TRD can bind and
326 recruit HDAC1 and LANA. In this way, unidirectional recruitment of HDAC1 and LANA only to DNA
327 bound MeCP2 is executed, while interaction with free MeCP2 is prevented (**Fig. 7**). On the contrary, HP1α
328 interacts with a different region, the N-terminus of MeCP2 that is available for binding also in its DNA-
329 free state, and therefore HP1α can recruit MeCP2. It has been shown that phosphorylation at serine 229
330 (pS229) of MeCP2 strongly enhances the interaction between MeCP2 and HP1α (10). Our observation that
331 HP1α can recruit MeCP2, may explain their observation that MeCP2 pS229 was enriched at the receptor
332 tyrosine kinase gene *RET* promoter.

333 Here we present only few examples of unidirectional recruitment. There are many cellular functions that
334 should be executed in a directional recruitment manner. The CRISPR-PITA we present in this study is a

335 convenient tool to ask these questions and has the potential to push forward our understanding of many
336 cellular functions.
337
338 **Materials and Methods**
339 **Cell culture**. SLK cells (kindly provided by Don Ganem & Rolf Renne) and NIH 3T3 cells (kindly provided
340 by Oren Kobiler) were cultured in Dulbecco's modified Eagle's medium (DMEM) supplemented with 10%
341 fetal bovine serum (heat inactivated) and 100 U/ml penicillin, 100 μg/ml streptomycin, 2 mM L-glutamine,
342 and 1 mM Sodium-Pyruvate in 5% CO_2 at 37°C. HCT and HCT Dnmt1-/- Dnmt3b -/- (DKO) cells (kindly
343 provided by Bert Vogelstein) were grown in McCoy's 5A medium supplemented with the above-mentioned
344 supplements. BJAB and BCBL1 cells (kindly provided by Richard F. Ambinder), and LCLs (kindly
345 provided by Uta Francke), were cultured in RPMI-1640 medium supplemented with 20% FBS and the
346 above-mentioned supplements. Single-cell derived clonal LCLs expressing the wt or mutant Rett syndrome
347 MeCP2 allele were established in the lab of Uta Francke (48).

348 **Plasmids**. pHRdSV40-dCas9-10xGCN4_v4-P2A-BFP (Addgene plasmid # 60903;
349 http://n2t.net/addgene:60903; RRID:Addgene_60903) and pHR-scFv-GCN4-sfGFP-GB1-dWPRE
350 (Addgene plasmid # 60907; http://n2t.net/addgene:60907; RRID:Addgene_60907) were a gift from Ron
351 Vale (31). pgRNA-humanized was a gift from Stanley Qi (Addgene plasmid # 44248;
352 http://n2t.net/addgene:44248; RRID:Addgene_44248) (25). The sgRNA targeting telomeres
353 (TTGGGTTAGGGTTAGGGTTAGGGTTAGTTTTAGAGCTAGAAATAGCAAGTTAAAATAAGGC
354 TAGTCCGTTATCAACTTGAAAAAGTGGCACCGAGTCGGTGCTTTTTTC) was cloned into
355 pgRNA-humanized. LANA, HDAC1, HP1α and MeCP2 were PCR amplified and cloned into pHR-scFv-
356 GCN4-sfGFP-GB1-dWPRE. Fc-LANA was further subcloned into pLIX_403, a gift from David Root
357 (Addgene plasmid # 41395; http://n2t.net/addgene:41395; RRID:Addgene_41395). pEGFP-c2 from
358 Clontech. GFP-LANA and LANA deletion plasmids were described previously (38, 62). For generation of
359 MeCP2 (T158M) mutation RNA was isolated from LCL 487 (T158M) cell line by Qiagen RNeasy mini kit
360 (cat no # 79656) and cDNA was prepared by maxima H minus first strand cDNA synthesis kit (cat no #
361 K1682). A fragment of MeCP2 containing the T158M mutation was amplified by PCR and cloned in
362 MeCP2-GFP plasmid (Addgene # 48078) and subsequently cloned into pHR-scFv-GCN4-sfGFP-GB1-
363 dWPRE plasmid. MBD domain deleted MeCP2 was created by overlap extension PCR. Oligomerization
364 mutant LANA was created by Q5 site directed mutagenesis kit (cat no# NEB E0554S). All primers can be
365 found in supplementary primer list (**Table S1**).

366 **Immunofluorescence assay**. $1X10^5$ cells were plated in 12 wells plate. Next day the cells were washed
367 once with PBS and were transfected using PolyJet In Vitro DNA Transfection Reagent (SignaGene
368 Laboratories Cat # SL100688) with the appropriate plasmids. In the day after $4X10^4$ cells were transferred
369 into chamber slide cell culture glass 8 wells (SPL life Science LTD). Next day, the cells were washed once
370 with PBS followed by fixation in 4% paraformaldehyde in PBS pH 7.4 for 10 minutes. After 3 washes with
371 PBS, cells were permeabilized for 10 min with PBS containing 0.25% Triton X-100. Cells were washed 3
372 times with PBS and blocked with 1% BSA, 22.52 mg/mL glycine in PBST (PBS+ 0.1% Tween 20) for 45
373 min in 37° C. The slides were incubated for 1 hour with primary antibodies, followed by 3 washes with
374 PBS. Then, the slides were incubated with secondary antibodies for 1 hour and washed again 3 times with
375 PBS and mounted with Vectaschield containing DAPI (Vector Laboratories, H-1500).

376 **Antibodies**. The following antibodies were used for immunofluorescence studies: Rat anti LANA
377 (Advanced Biotechnologies, cat#13-210-100), Mouse anti LANA (Leica, NCL-HHV8-LNA), Mouse anti
378 TRF2 (Merck, 05-521), Rabbit anti MeCP2 (Abcam, ab2828), Rabbit anti mSin3a/SIN3A (Abcam,
379 ab3479), Mouse anti HA (Sigma H9658), Mouse anti ORC2 (MBL Life Science, M055-3), and Rabbit anti
380 HDAC1 (Abcam, ab53091). Goat anti rabbit Alexa 488 (Abcam, ab150077), Goat anti Rat Alexa 488
381 (Abcam, ab150157), and Goat anti Mouse Alexa 594 (Abcam, ab150116). Fc-MeCP2, Fc-HP1α, and Fc-
382 HDAC1 were detected with Mouse anti HA. Fc-LANA was detected by Mouse anti LANA, except in
383 combination with TRF2 where Rat anti LANA was used. FLAG-LANA mutants (N+C, N, C) were detected
384 with Rabbit anti FLAG (Sigma 7425).

385 **Confocal imaging.** Images were captured with Zeiss LSM780 inverted confocal microscope through a 63X
386 objective with Z stack mode. Then, the middle stacks were selected and merged using Subset mode and
387 Maximum Intensity Projection mode, respectively with Zenn software black edition. Processing and
388 exporting of the resulted images was done with Zenn software blue edition.

389 **Dot Quantification**. Merged stacks images were analyzed with FIJI software as follow: Signal exposure
390 of loaded images was set using the Threshold mode to the point that clear separated dots were seen, followed
391 by Watershed mode, in order to fine tune the separation of the dots. Then, Region of Interest was selected,
392 and measurements were directed to the appropriate channel. Area size in $micron^2$ of the dots was collected
393 using Analyze Particles mode for each and every selected cell.

394 **LCL infection and maintenance assay**. LCLs were infected with KSHV by co-culture (63). Briefly, Vero-
395 rKSHV.219 cells (45) were induced with 1.25 mM sodium butyrate and 20 ng/ml 12-*O*-
396 tetradecanoylphorbol-13-acetate (TPA) and after 48 h were cocultured with LCL cells (1:1 cell ratio) in

397 RPMI 1640 medium for an additional 48 h. Medium containing the LCLs infected cells was collected and
398 transferred to a new flask for an additional 48 h. Transferred again to a new flask, and at days 2, 7, 14, 24,
399 cells were taken for FACS analysis to detect the number of GFP positive cells. At the same time points,
400 genomic DNA was isolated from with DNeasy blood and tissue kit (cat no # 69506) as per manufacturer
401 instructions. Real time PCR was performed on genomic DNA using Fast SYBR green master
402 mix (Applied Biosystems), and results were analyzed with a CFX96 Touch real-time PCR
403 detection system (Bio-Rad). GAPDH was used as an internal control.

404 **Acknowledgments**

405 We would like to thank J Ron Vale, Stanley Qi, David Root, and S. Diane Hayward for kindly providing
406 plasmids, and Don Ganem, Rolf Renne, Oren Kobiler, Richard F. Ambinder, Bert Vogelstein and Uta
407 Francke for cell lines. We also would like to thank S. Diane Hayward for critically reading the manuscript,
408 and Yosef Shaul for fruitful discussions. We are grateful for the support of the Elias, Genevieve and
409 Georgianna Atol Charitable Trust to the Daniella Lee Casper Laboratory in Viral Oncology. This work was
410 supported by grants from the Israel Science Foundation (https://www.isf.org.il) to M.S. (1134/16), and
411 Research Career Development Award from the Israel Cancer Research Fund (https://www.icrfonline.org/)
412 to M.S. (01282). The funders had no role in study design, data collection and analysis, decision to publish,
413 or preparation of the manuscript.

414

415 **References**

416 1. Hall JM, McDonnell DP, Korach KS. Allosteric regulation of estrogen receptor structure,
417 function, and coactivator recruitment by different estrogen response elements. Molecular
418 endocrinology (Baltimore, Md. 2002;16(3):469-86.
419 2. Kim TK, Maniatis T. The mechanism of transcriptional synergy of an in vitro assembled
420 interferon-beta enhanceosome. Molecular cell. 1997;1(1):119-29.
421 3. Merika M, Williams AJ, Chen G, Collins T, Thanos D. Recruitment of CBP/p300 by the
422 IFN beta enhanceosome is required for synergistic activation of transcription. Molecular cell.
423 1998;1(2):277-87.
424 4. Nan X, Campoy FJ, Bird A. MeCP2 is a transcriptional repressor with abundant binding
425 sites in genomic chromatin. Cell. 1997;88(4):471-81.
426 5. Jones PL, Veenstra GJ, Wade PA, Vermaak D, Kass SU, Landsberger N, et al. Methylated
427 DNA and MeCP2 recruit histone deacetylase to repress transcription. Nature genetics.
428 1998;19(2):187-91.
429 6. Nan X, Ng HH, Johnson CA, Laherty CD, Turner BM, Eisenman RN, et al. Transcriptional
430 repression by the methyl-CpG-binding protein MeCP2 involves a histone deacetylase complex.
431 Nature. 1998;393(6683):386-9.

432 7. Bannister AJ, Zegerman P, Partridge JF, Miska EA, Thomas JO, Allshire RC, et al.
433 Selective recognition of methylated lysine 9 on histone H3 by the HP1 chromo domain. Nature.
434 2001;410(6824):120-4.
435 8. Lachner M, O'Carroll D, Rea S, Mechtler K, Jenuwein T. Methylation of histone H3 lysine
436 9 creates a binding site for HP1 proteins. Nature. 2001;410(6824):116-20.
437 9. Agarwal N, Hardt T, Brero A, Nowak D, Rothbauer U, Becker A, et al. MeCP2 interacts
438 with HP1 and modulates its heterochromatin association during myogenic differentiation. Nucleic
439 acids research. 2007;35(16):5402-8.
440 10. Gonzales ML, Adams S, Dunaway KW, LaSalle JM. Phosphorylation of distinct sites in
441 MeCP2 modifies cofactor associations and the dynamics of transcriptional regulation. Molecular
442 and cellular biology. 2012;32(14):2894-903.
443 11. Chang Y, Cesarman E, Pessin MS, Lee F, Culpepper J, Knowles DM, et al. Identification
444 of herpesvirus-like DNA sequences in AIDS-associated Kaposi's sarcoma. Science (New York,
445 NY. 1994;266(5192):1865-9.
446 12. Henke-Gendo C, Schulz TF. Transmission and disease association of Kaposi's sarcoma-
447 associated herpesvirus: recent developments. Curr Opin Infect Dis. 2004;17(1):53-7.
448 13. Ye F, Lei X, Gao SJ. Mechanisms of Kaposi's Sarcoma-Associated Herpesvirus Latency
449 and Reactivation. Adv Virol. 2011;2011.
450 14. Rainbow L, Platt GM, Simpson GR, Sarid R, Gao SJ, Stoiber H, et al. The 222- to 234-
451 kilodalton latent nuclear protein (LNA) of Kaposi's sarcoma-associated herpesvirus (human
452 herpesvirus 8) is encoded by orf73 and is a component of the latency-associated nuclear antigen.
453 J Virol. 1997;71(8):5915-21.
454 15. Kedes DH, Lagunoff M, Renne R, Ganem D. Identification of the gene encoding the major
455 latency-associated nuclear antigen of the Kaposi's sarcoma-associated herpesvirus. J Clin Invest.
456 1997;100(10):2606-10.
457 16. Grundhoff A, Ganem D. The latency-associated nuclear antigen of Kaposi's sarcoma-
458 associated herpesvirus permits replication of terminal repeat-containing plasmids. J Virol.
459 2003;77(4):2779-83.
460 17. Hu J, Garber AC, Renne R. The latency-associated nuclear antigen of Kaposi's sarcoma-
461 associated herpesvirus supports latent DNA replication in dividing cells. J Virol.
462 2002;76(22):11677-87.
463 18. Kelley-Clarke B, De Leon-Vazquez E, Slain K, Barbera AJ, Kaye KM. Role of Kaposi's
464 sarcoma-associated herpesvirus C-terminal LANA chromosome binding in episome persistence. J
465 Virol. 2009;83(9):4326-37.
466 19. De Leon Vazquez E, Kaye KM. The internal Kaposi's sarcoma-associated herpesvirus
467 LANA regions exert a critical role on episome persistence. J Virol. 2011;85(15):7622-33.
468 20. Hellert J, Weidner-Glunde M, Krausze J, Lünsdorf H, Ritter C, Schulz TF, et al. The 3D
469 structure of Kaposi sarcoma herpesvirus LANA C-terminal domain bound to DNA. Proceedings
470 of the National Academy of Sciences of the United States of America. 2015;112(21):6694-9.
471 21. Garber AC, Hu J, Renne R. Latency-associated nuclear antigen (LANA) cooperatively
472 binds to two sites within the terminal repeat, and both sites contribute to the ability of LANA to
473 suppress transcription and to facilitate DNA replication. J Biol Chem. 2002;277(30):27401-11.
474 22. Domsic JF, Chen HS, Lu F, Marmorstein R, Lieberman PM. Molecular basis for
475 oligomeric-DNA binding and episome maintenance by KSHV LANA. PLoS Pathog.
476 2013;9(10):e1003672.

477 23. De Leo A, Deng Z, Vladimirova O, Chen HS, Dheekollu J, Calderon A, et al. LANA
478 oligomeric architecture is essential for KSHV nuclear body formation and viral genome
479 maintenance during latency. PLoS Pathog. 2019;15(1):e1007489.
480 24. Jinek M, Chylinski K, Fonfara I, Hauer M, Doudna JA, Charpentier E. A programmable
481 dual-RNA-guided DNA endonuclease in adaptive bacterial immunity. Science (New York, NY.
482 2012;337(6096):816-21.
483 25. Qi LS, Larson MH, Gilbert LA, Doudna JA, Weissman JS, Arkin AP, et al. Repurposing
484 CRISPR as an RNA-guided platform for sequence-specific control of gene expression. Cell.
485 2013;152(5):1173-83.
486 26. Gilbert LA, Larson MH, Morsut L, Liu Z, Brar GA, Torres SE, et al. CRISPR-mediated
487 modular RNA-guided regulation of transcription in eukaryotes. Cell. 2013;154(2):442-51.
488 27. Deng W, Shi X, Tjian R, Lionnet T, Singer RH. CASFISH: CRISPR/Cas9-mediated in situ
489 labeling of genomic loci in fixed cells. Proceedings of the National Academy of Sciences of the
490 United States of America. 2015;112(38):11870-5.
491 28. Chen B, Gilbert LA, Cimini BA, Schnitzbauer J, Zhang W, Li GW, et al. Dynamic imaging
492 of genomic loci in living human cells by an optimized CRISPR/Cas system. Cell.
493 2013;155(7):1479-91.
494 29. Anton T, Bultmann S, Leonhardt H, Markaki Y. Visualization of specific DNA sequences
495 in living mouse embryonic stem cells with a programmable fluorescent CRISPR/Cas system.
496 Nucleus. 2014;5(2):163-72.
497 30. Duan J, Lu G, Hong Y, Hu Q, Mai X, Guo J, et al. Live imaging and tracking of genome
498 regions in CRISPR/dCas9 knock-in mice. Genome Biol. 2018;19(1):192.
499 31. Tanenbaum ME, Gilbert LA, Qi LS, Weissman JS, Vale RD. A protein-tagging system for
500 signal amplification in gene expression and fluorescence imaging. Cell. 2014;159(3):635-46.
501 32. Ballestas ME, Chatis PA, Kaye KM. Efficient persistence of extrachromosomal KSHV
502 DNA mediated by latency-associated nuclear antigen. Science (New York, NY.
503 1999;284(5414):641-4.
504 33. Kelley-Clarke B, Ballestas ME, Srinivasan V, Barbera AJ, Komatsu T, Harris TA, et al.
505 Determination of Kaposi's sarcoma-associated herpesvirus C-terminal latency-associated nuclear
506 antigen residues mediating chromosome association and DNA binding. J Virol. 2007;81(8):4348-
507 56.
508 34. Hellert J, Weidner-Glunde M, Krausze J, Richter U, Adler H, Fedorov R, et al. A structural
509 basis for BRD2/4-mediated host chromatin interaction and oligomer assembly of Kaposi sarcoma-
510 associated herpesvirus and murine gammaherpesvirus LANA proteins. PLoS Pathog.
511 2013;9(10):e1003640.
512 35. Chiu YF, Sugden AU, Fox K, Hayes M, Sugden B. Kaposi's sarcoma-associated
513 herpesvirus stably clusters its genomes across generations to maintain itself extrachromosomally.
514 The Journal of cell biology. 2017;216(9):2745-58.
515 36. Stedman W, Deng Z, Lu F, Lieberman PM. ORC, MCM, and Histone Hyperacetylation at
516 the Kaposi's Sarcoma-Associated Herpesvirus Latent Replication Origin. J Virol.
517 2004;78(22):12566-75.
518 37. Verma SC, Lan K, Choudhuri T, Cotter MA, Robertson ES. An autonomous replicating
519 element within the KSHV genome. Cell host & microbe. 2007;2(2):106-18.

520 38. Krithivas A, Young DB, Liao G, Greene D, Hayward SD. Human herpesvirus 8 LANA
521 interacts with proteins of the mSin3 corepressor complex and negatively regulates Epstein-Barr
522 virus gene expression in dually infected PEL cells. J Virol. 2000;74(20):9637-45.
523 39. Cai Q, Cai S, Zhu C, Verma SC, Choi JY, Robertson ES. A unique SUMO-2-interacting
524 motif within LANA is essential for KSHV latency. PLoS Pathog. 2013;9(11):e1003750.
525 40. Krithivas A, Fujimuro M, Weidner M, Young DB, Hayward SD. Protein interactions
526 targeting the latency-associated nuclear antigen of Kaposi's sarcoma-associated herpesvirus to cell
527 chromosomes. J Virol. 2002;76(22):11596-604.
528 41. Matsumura S, Persson LM, Wong L, Wilson AC. The latency-associated nuclear antigen
529 interacts with MeCP2 and nucleosomes through separate domains. J Virol. 2010;84(5):2318-30.
530 42. Verma SC, Cai Q, Kreider E, Lu J, Robertson ES. Comprehensive analysis of LANA
531 interacting proteins essential for viral genome tethering and persistence. PloS one.
532 2013;8(9):e74662.
533 43. Stuber G, Mattsson K, Flaberg E, Kati E, Markasz L, Sheldon JA, et al. HHV-8 encoded
534 LANA-1 alters the higher organization of the cell nucleus. Molecular cancer. 2007;6:28.
535 44. Rhee I, Bachman KE, Park BH, Jair KW, Yen RW, Schuebel KE, et al. DNMT1 and
536 DNMT3b cooperate to silence genes in human cancer cells. Nature. 2002;416(6880):552-6.
537 45. Barbera AJ, Chodaparambil JV, Kelley-Clarke B, Joukov V, Walter JC, Luger K, et al. The
538 Nucleosomal Surface as a Docking Station for Kaposi's Sarcoma Herpesvirus LANA. Science
539 (New York, NY. 2006;311(5762):856-61.
540 46. Viejo-Borbolla A, Ottinger M, Bruning E, Burger A, Konig R, Kati E, et al. Brd2/RING3
541 interacts with a chromatin-binding domain in the Kaposi's Sarcoma-associated herpesvirus
542 latency-associated nuclear antigen 1 (LANA-1) that is required for multiple functions of LANA-
543 1. J Virol. 2005;79(21):13618-29.
544 47. Ghosh RP, Horowitz-Scherer RA, Nikitina T, Gierasch LM, Woodcock CL. Rett
545 syndrome-causing mutations in human MeCP2 result in diverse structural changes that impact
546 folding and DNA interactions. J Biol Chem. 2008;283(29):20523-34.
547 48. Traynor J, Agarwal P, Lazzeroni L, Francke U. Gene expression patterns vary in clonal
548 cell cultures from Rett syndrome females with eight different MECP2 mutations. BMC Med
549 Genet. 2002;3:12.
550 49. Griffiths R, Whitehouse A. Herpesvirus saimiri episomal persistence is maintained via
551 interaction between open reading frame 73 and the cellular chromosome-associated protein
552 MeCP2. J Virol. 2007;81(8):4021-32.
553 50. Dedon PC, Soults JA, Allis CD, Gorovsky MA. A simplified formaldehyde fixation and
554 immunoprecipitation technique for studying protein-DNA interactions. Anal Biochem.
555 1991;197(1):83-90.
556 51. Orlando V, Paro R. Mapping Polycomb-repressed domains in the bithorax complex using
557 in vivo formaldehyde cross-linked chromatin. Cell. 1993;75(6):1187-98.
558 52. Aronheim A, Zandi E, Hennemann H, Elledge SJ, Karin M. Isolation of an AP-1 repressor
559 by a novel method for detecting protein-protein interactions. Molecular and cellular biology.
560 1997;17(6):3094-102.
561 53. Gonzalez-Serricchio AS, Sternberg PW. Visualization of C. elegans transgenic arrays by
562 GFP. BMC Genet. 2006;7:36.

563 54. Higa M, Kushiyama T, Kurashige S, Kohmon D, Enokitani K, Iwahori S, et al. TRF2
564 recruits ORC through TRFH domain dimerization. Biochim Biophys Acta Mol Cell Res.
565 2017;1864(1):191-201.
566 55. Gao Y, Han M, Shang S, Wang H, Qi LS. Interrogation of the dynamic properties of higher-
567 order heterochromatin using CRISPR-dCas9. Molecular cell. 2021.
568 56. Shin Y, Chang YC, Lee DSW, Berry J, Sanders DW, Ronceray P, et al. Liquid Nuclear
569 Condensates Mechanically Sense and Restructure the Genome. Cell. 2018;175(6):1481-91 e13.
570 57. Vladimirova O, De Leo A, Deng Z, Wiedmer A, Hayden J, Lieberman PM. Phase
571 separation and DAXX redistribution contribute to LANA nuclear body and KSHV genome
572 dynamics during latency and reactivation. PLoS Pathog. 2021;17(1):e1009231.
573 58. Wang L, Hu M, Zuo MQ, Zhao J, Wu D, Huang L, et al. Rett syndrome-causing mutations
574 compromise MeCP2-mediated liquid-liquid phase separation of chromatin. Cell Res.
575 2020;30(5):393-407.
576 59. Calderwood M, White RE, Griffiths RA, Whitehouse A. Open reading frame 73 is required
577 for herpesvirus saimiri A11-S4 episomal persistence. J Gen Virol. 2005;86(Pt 10):2703-8.
578 60. Adams VH, McBryant SJ, Wade PA, Woodcock CL, Hansen JC. Intrinsic disorder and
579 autonomous domain function in the multifunctional nuclear protein, MeCP2. J Biol Chem.
580 2007;282(20):15057-64.
581 61. Ghosh RP, Horowitz-Scherer RA, Nikitina T, Shlyakhtenko LS, Woodcock CL. MeCP2
582 binds cooperatively to its substrate and competes with histone H1 for chromatin binding sites.
583 Molecular and cellular biology. 2010;30(19):4656-70.
584 62. Fujimuro M, Hayward SD. The latency-associated nuclear antigen of Kaposi's sarcoma-
585 associated herpesvirus manipulates the activity of glycogen synthase kinase-3beta. J Virol.
586 2003;77(14):8019-30.
587 63. Myoung J, Ganem D. Infection of lymphoblastoid cell lines by Kaposi's sarcoma-
588 associated herpesvirus: critical role of cell-associated virus. J Virol. 2011;85(19):9767-77.
589
590
591
592
593
594
595
596
597
598
599
600

601 **Figure legends**

602 **Figure 1. Schematic illustration of CRISPR-PITA. (A)** Schematic illustration of dCas9-SunTag, sgRNA
603 and Fc-LANA or other protein of interest (Fc-pY), and their binding to repetitive elements. **(B)** SLK cells
604 were transfected with dCas9-SunTag, Fc-LANA, and sgTelomere as illustrated on the left of the images.
605 Immunofluorescence assay was performed to detect LANA (red), and the nucleus was stained with DAPI
606 (blue). Scale bar = 5 μm. **(C)** Schematic illustration of the CRISPR-PITA, targeting of Fc-LANA or any
607 other protein of interest to the telomeres via dCas9. Then the recruitment of other nuclear proteins to these
608 dots is evaluated via immunostaining.

609 **Figure 2. LANA recruits ORC2 and SIN3A but not MeCP2.** SLK cells were transfected with dCas9-
610 SunTag, Fc-LANA, and sgTelomere expression plasmids as can be seen in the illustrations on the left.
611 Immunofluorescence assays were performed to detect LANA (red) and ORC2 **(A)** mSin3a **(B)** or MeCP2
612 **(C)** (in green) cellular localization. The nucleus was stained with DAPI. Scale bar = 5 μm. The average
613 ratio between big and small foci for each analysed protein is presented on the right, based on the threshold
614 $\geq$0.15 micron^2, (n=15). One-tailed T-tests were performed on the ratios (*, $P \leq 0.05$; **, $P \leq 0.01$, ***, $P \leq$
615 0.001). Results are presented as mean +/- SD.

616 **Figure 3. MeCP2 recruits LANA.** SLK cells were transfected with dCas9-SunTag, Fc-MeCP2, and
617 sgTelomere in combination with GFP-LANA **(A)** or GFP **(B)** as illustrated on the left. Immunofluorescence
618 assay was performed to detect Fc-MeCP2, or fluorescently labelled GFP-LANA and GFP. The nucleus was
619 stained with DAPI. Scale bar = 5 μm. The average ratio between big and small foci are presented on the
620 right, same as in Fig 2. (C) SLK cells were transfected with FLAG-LANA N+C, FLAG-LANA C, or
621 FLAG-LANA N, same as in A. Immunofluorescence assay was performed to detect both Fc-MeCP2 and
622 LANA.

623 **Figure 4. MeCP2 recruits HDAC1, while HDAC1 cannot recruit MeCP2. (A)** HCT cells were
624 transfected with dCas9-SunTag, Fc-MeCP2 and sgTelomere as illustrated on the left. Immunofluorescence
625 assay was performed to detect HDAC1 (green) and Fc-MeCP2 (red). **(B-C) HCT (B)** and HCT DKO **(C)**
626 cells were transfected same as in A but with Fc-HDAC1. Immunofluorescence assay was performed to
627 detect MeCP2 (green) and Fc-HDAC1 (red). The nucleus was stained with DAPI. Scale bar = 5 μm. The
628 average ratio between big and small foci are presented on the right, same as in Fig 2.

629 **Figure 5. HP1α recruits MeCP2.** SLK cells were transfected with dCas9-SunTag, Fc-HP1α, and
630 sgTelomere as illustrated on the left. Immunofluorescence assay was performed to detect MeCP2 (green)

631 and Fc-HP1α (red). The nucleus was stained with DAPI. Scale bar = 5 μm. The average ratio between big
632 and small foci are presented on the right, same as in Fig 2.

633 **Figure 6. Rett syndrome mutant MeCP2 T158M cannot support KSHV latency. (A-B)** LCLs were
634 infected with rKSHV.219 and GFP-positive cells by FACS analysis (**A**) or amount of KSHV DNA by
635 qPCR (**B**) were evaluated at the indicated time points. Experiment was performed with biological
636 triplicates. (**C**) Immunofluorescence assay was performed to detect GFP-LANA (green) and Fc- MeCP2
637 (red). The nucleus was stained with DAPI. Scale bar = 5 μm. The average ratio between big and small foci
638 are presented on the right, same as in Fig 2. (**D**) NIH 3T3 cells were transfected with GFP-LANA and wt
639 MeCP2, T158M mutant, or del-MBD. Immunofluorescence assay was performed same as in C. Intensity
640 profiles along the indicated arrows are presented on the right.

641 **Figure 7. Schematic presentation of directional recruitment. (A)** In its DNA free form, the MBD and
642 TRD of MeCP2 are not available for LANA interaction. **(B)** Upon binding to methylated DNA LANA
643 binding surface in MeCP2 becomes available for LANA binding. **(C)** LANA tethers the viral episomal
644 genomes to cellular chromosomes by binding to histones via its N-terminal domain and to MeCP2 via its
645 C-terminal domain. This unidirectional recruitment of LANA by MeCP2 is essential for viral genome
646 maintenance during latency.

647

648

649

650

651

652

653

654

655

656

657 **Supplementary figure legends**

658 **FIG S1. LANA-telomere dots co-localize with the telomeric protein TRF2.** SLK cells were transfected
659 with dCas9-SunTag, Fc-LANA (**A & B**) or Fc-LANA oligomerization mutant (**B**), and sgTelomere as
660 illustrated on the left of the images. Immunofluorescence assay was performed to detect LANA (red) and
661 TRF2 (white), and the nucleus was stained with DAPI. Scale bar = 5 μm.

662 **FIG S2. Fc-LANA interacts with MeCP2.** HEK 293T cells were co-transfected with Fc-LANA (Fc-
663 FLAG-LANA) and MeCP2 expression vectors. 48 h after transfection cells were lysed in lysis buffer
664 (50mM Tris-HCl pH 7.9; 100mM NaCl; 0.5mM EDTA; 2% Glycerol; 0.2% NP40 and Protease
665 inhibitor cocktail (Halt™ Protease Inhibitor Cocktail (100X) Thermo Scientific™). Cell extracts were
666 immunoprecipitated with anti-FLAG beads and subjected to SDS-PAGE and Western blot analysis with
667 anti-MeCP2 (upper and lower panels), or anti-FLAG (middle panel) antibodies.

668 **FIG S3. LANA cannot recruit MeCP2 even in HCT-DKO cells.** HCT116 **(A)** and DKO (DNMT3B -/-
669 and DNMT1 -/-) HCT116 cells **(B)** were transfected with dCas9-SunTag, Fc-LANA, and sgTelomere as
670 illustrated on the left of the images. Immunofluorescence assay was performed to detect MeCP2 (green)
671 and LANA (red). The nucleus was stained with DAPI. Scale bar = 5 μm.

672 **FIG S4. ORC2 and SIN3A but not MeCP2 co-localize with LANA dots in KSHV infected cells.**
673 Immunofluorescence assays were performed to detect ORC2 **(A)** SIN3A **(B)** or MeCP2 **(C)** and LANA
674 (red) cellular localization in KSHV-negative (BJAB) and KSHV-positive (BCBL1) lymphoma cell lines.
675 The nucleus was stained with DAPI. Scale bar = 5 μm.

676 **Table S1. Primers used in this study.**

677

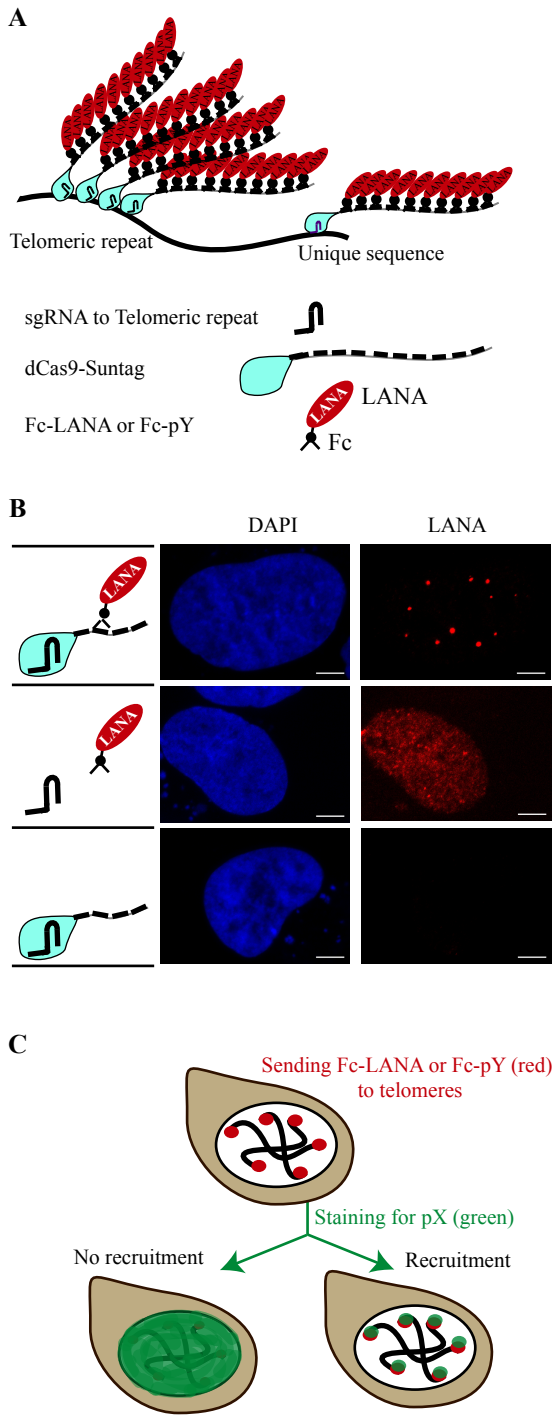

Figure 1. Schematic illustration of CRISPR-PITA. (**A**) Schematic illustration of dCas9-SunTag, sgRNA and Fc-LANA or other protein of interest (Fc-pY), and their binding to repetitive elements. (**B**) SLK cells were transfected with dCas9-SunTag, Fc-LANA, and sgTelomere as illustrated on the left of the images. Immunofluorescence assay was performed to detect LANA (red), and the nucleus was stained with DAPI (blue). Scale bar = 5 µm. (**C**) Schematic illustration of the CRISPR-PITA, targeting of Fc-LANA or any other protein of interest to the telomeres via dCas9. Then the recruitment of other nuclear proteins to these dots is evaluated via immunostaining.

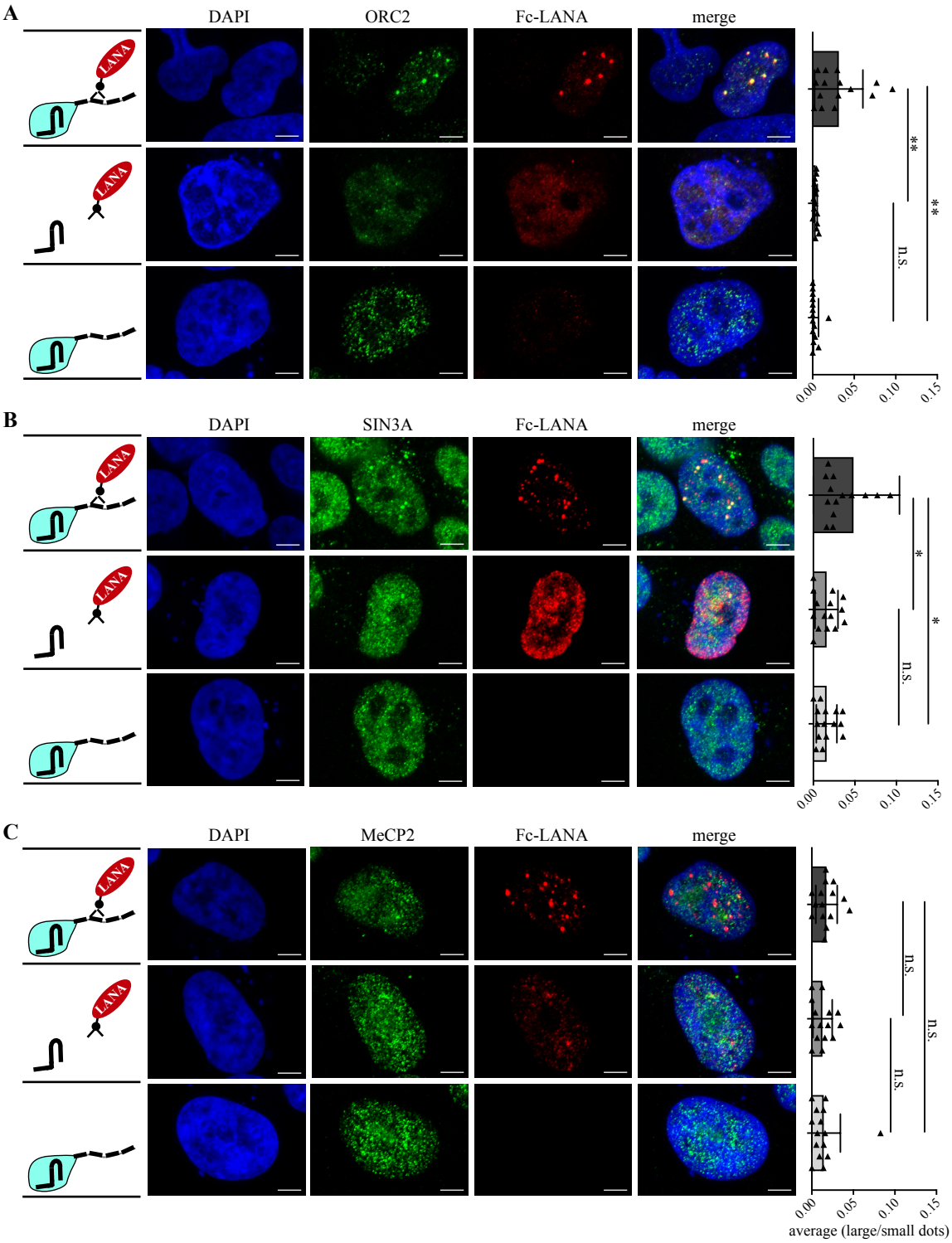

Figure 2. LANA recruits ORC2 and SIN3A but not MeCP2. SLK cells were transfected with dCas9-SunTag, Fc-LANA, and sgTelomere expression plasmids as can be seen in the illustrations on the left. Immunofluorescence assays were performed to detect LANA (red) and ORC2 **(A)** mSin3a **(B)** or MeCP2 **(C)** (in green) cellular localization. The nucleus was stained with DAPI. Scale bar = 5 µm. The average ratio between big and small foci for each analysed protein is presented on the right, based on the threshold ≥0.15 micron², (n=15). One-tailed T-tests were performed on the ratios (*, $P \leq 0.05$; **, $P \leq 0.01$, ***, $P \leq 0.001$). Results are presented as mean +/- SD.

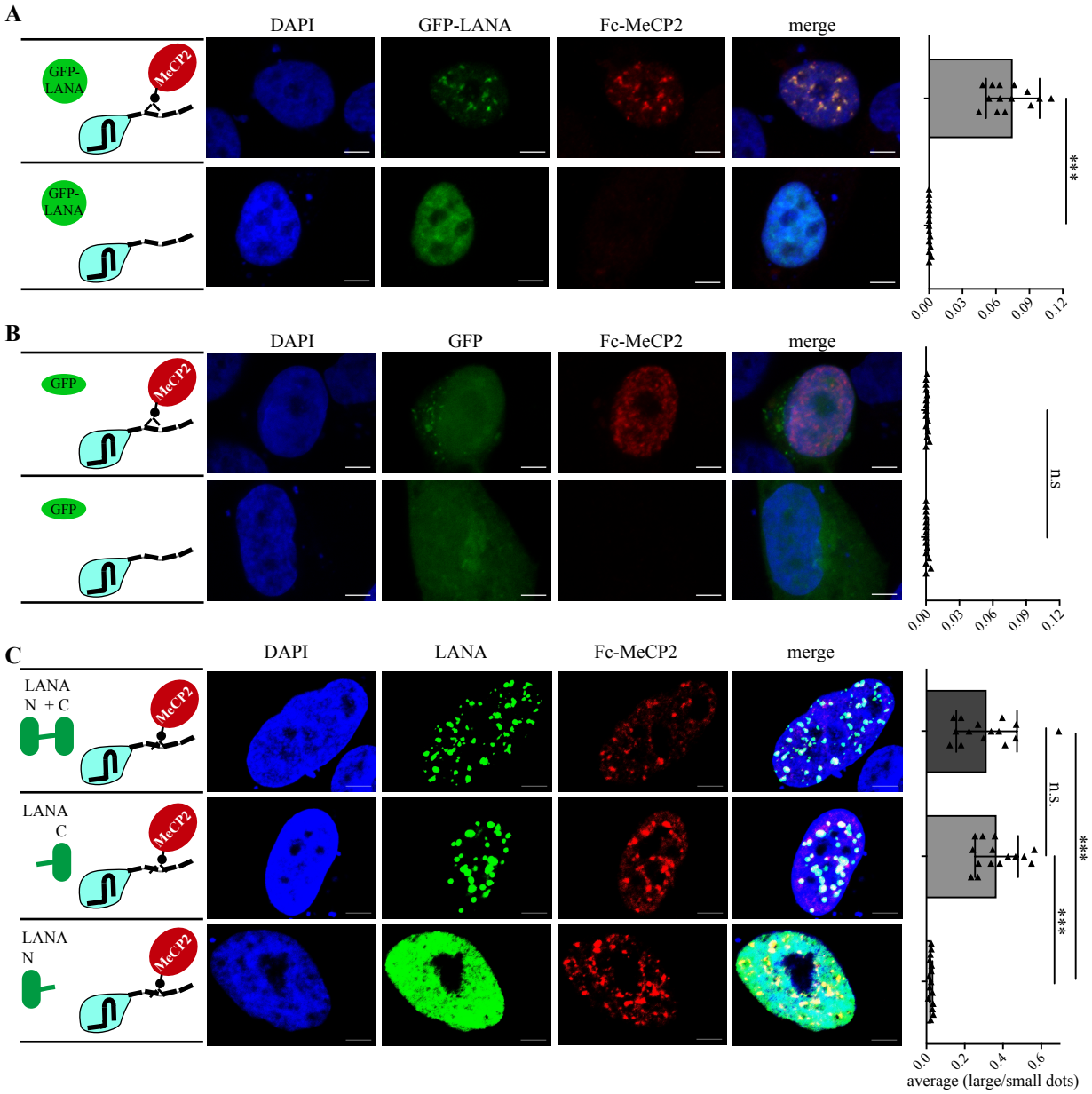

Figure 3. MeCP2 recruits LANA. SLK cells were transfected with dCas9-SunTag, Fc-MeCP2, and sgTelomere in combination with GFP-LANA (**A**) or GFP (**B**) as illustrated on the left. Immunofluorescence assay was performed to detect Fc-MeCP2, or fluorescently labelled GFP-LANA and GFP. The nucleus was stained with DAPI. Scale bar = 5 µm. The average ratio between big and small foci are presented on the right, same as in Fig 2. (**C**) SLK cells were transfected with FLAG-LANA N+C, FLAG-LANA C, or FLAG-LANA N, same as in A. Immunofluorescence assay was performed to detect both Fc-MeCP2 and LANA.

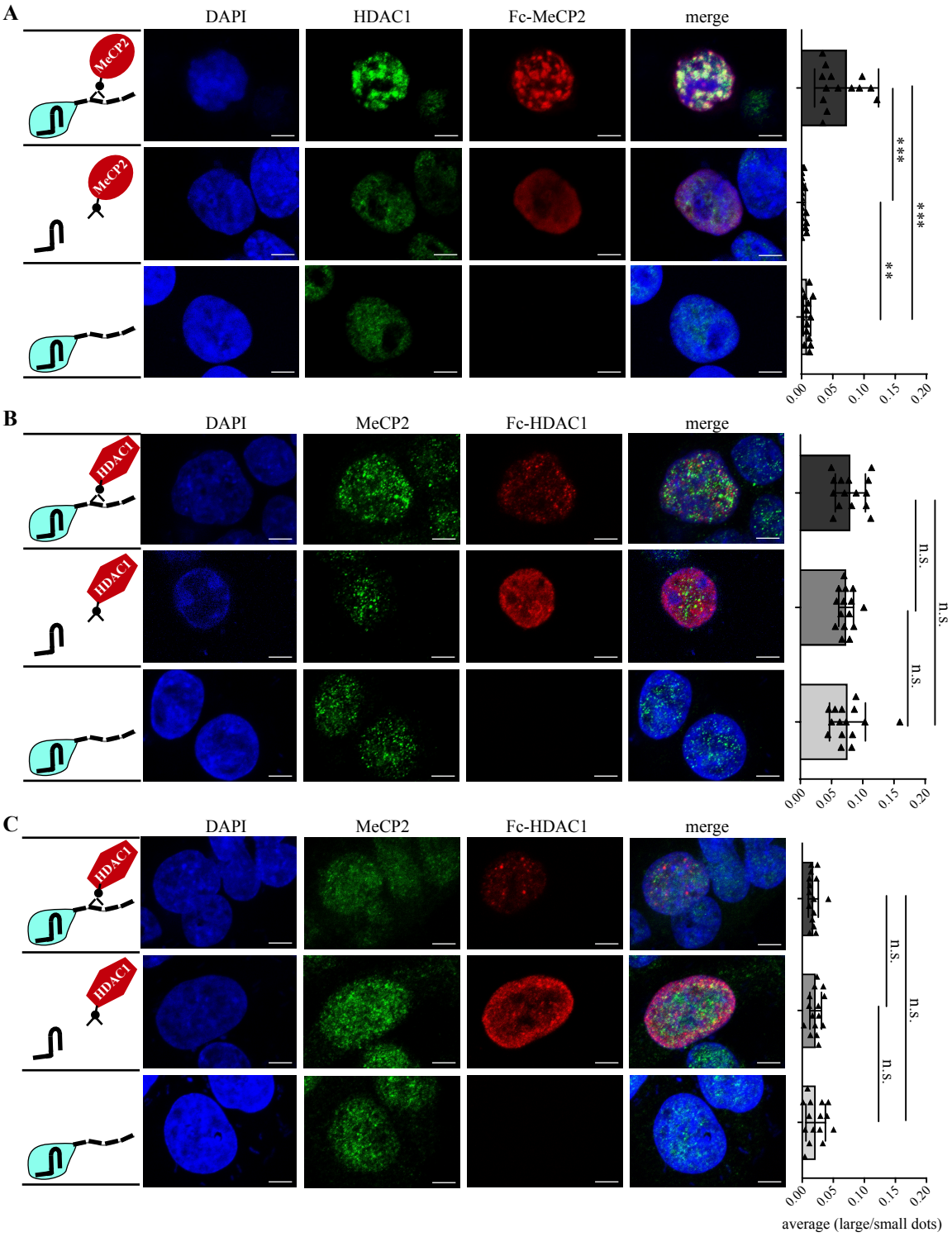

Figure 4. MeCP2 recruits HDAC1, while HDAC1 cannot recruit MeCP2. (A) HCT cells were transfected with dCas9-SunTag, Fc-MeCP2 and sgTelomere as illustrated on the left. Immunofluorescence assay was performed to detect HDAC1 (green) and Fc-MeCP2 (red). (**B-C**) HCT (**B**) and HCT DKO (**C**) cells were transfected same as in A but with Fc-HDAC1. Immunofluorescence assay was performed to detect MeCP2 (green) and Fc-HDAC1 (red). The nucleus was stained with DAPI. Scale bar = 5 μm. The average ratio between big and small foci are presented on the right, same as in Fig 2.

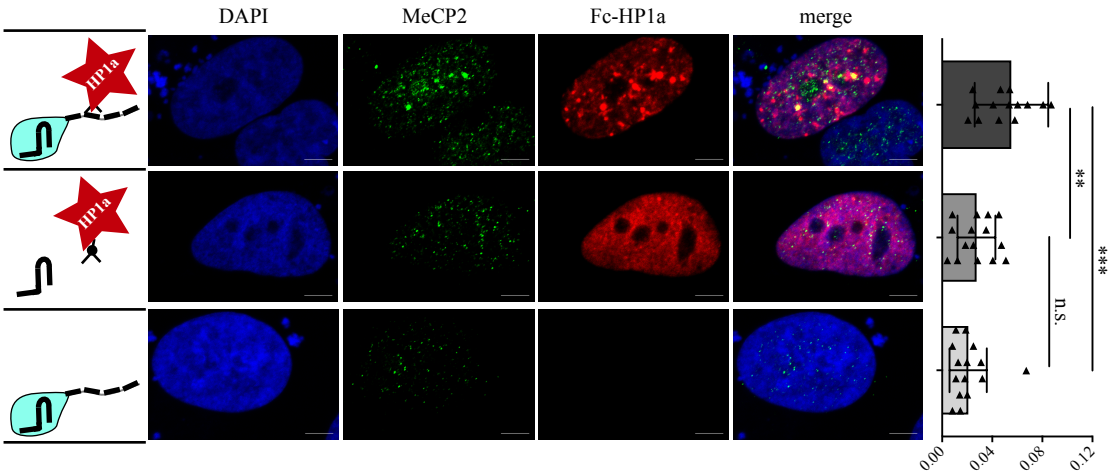

Figure 5. HP1α recruits MeCP2. SLK cells were transfected with dCas9-SunTag, Fc-HP1α, and sgTelomere as illustrated on the left. Immunofluorescence assay was performed to detect MeCP2 (green) and Fc-HP1α (red). The nucleus was stained with DAPI. Scale bar = 5 μm. The average ratio between big and small foci are presented on the right, same as in Fig 2.

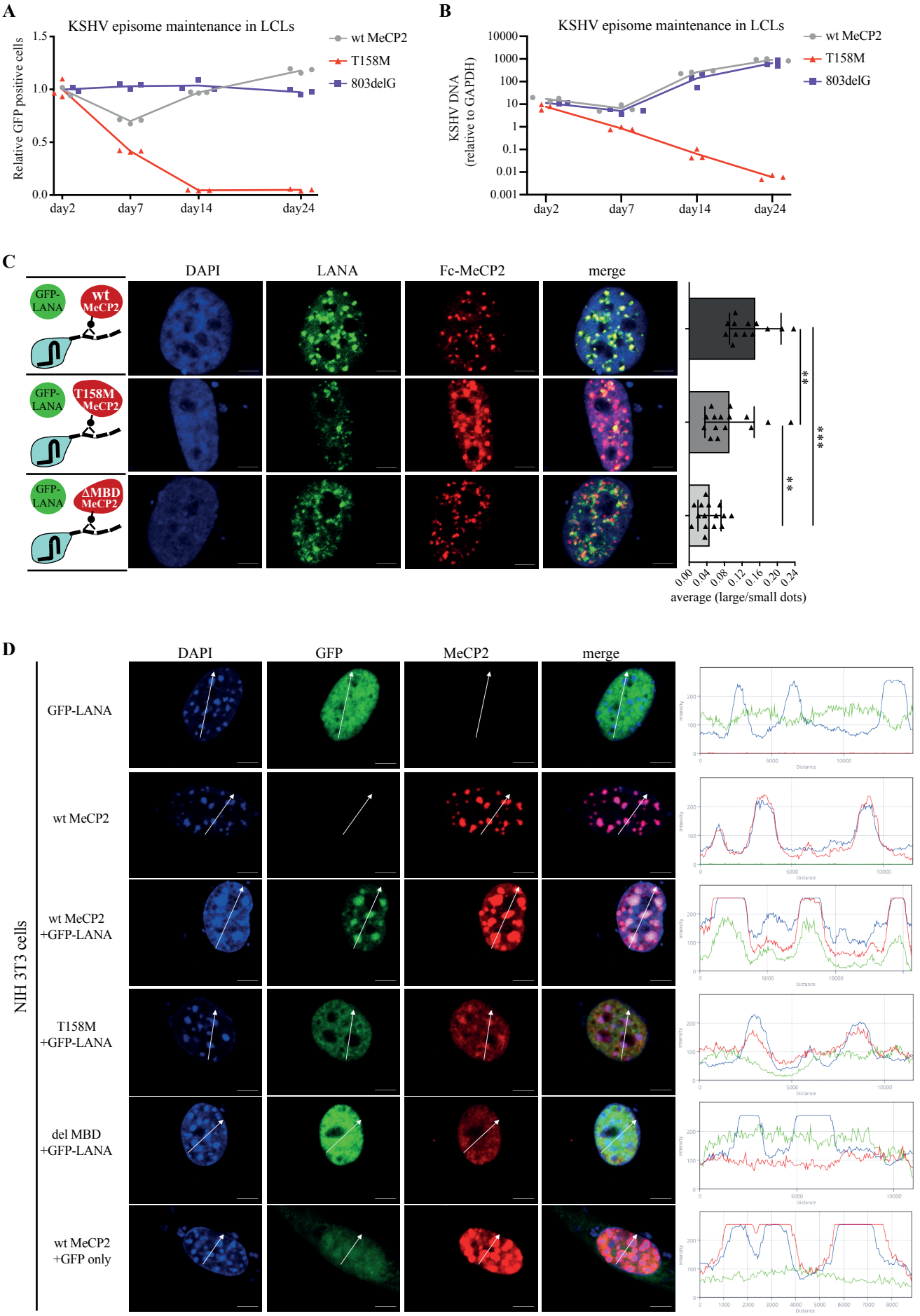
A
KSHV episome maintenance in LCLs
Relative GFP positive cells
1.5
1.0
0.5
0.0
day2
day7
day14
day24
wt MeCP2
T158M
803delG
B
KSHV episome maintenance in LCLs
KSHV DNA (relative to GAPDH)
10000
1000
100
10
1
0.1
0.01
0.001
day2
day7
day14
day24
wt MeCP2
T158M
803delG
C
DAPI
LANA
Fc-MeCP2
merge
GFP-LANA
wt MeCP2
T158M MeCP2
ΔMBD MeCP2
**
***
**
0.00
0.04
0.08
0.12
0.16
0.20
0.24
average (large/small dots)
D
DAPI
GFP
MeCP2
merge
NIH 3T3 cells
GFP-LANA
wt MeCP2
wt MeCP2 +GFP-LANA
T158M +GFP-LANA
del MBD +GFP-LANA
wt MeCP2 +GFP only

Legend to Figure 6 on previous page

Figure 6. Rett syndrome mutant MeCP2 T158M cannot support KSHV latency. (**A-B**) LCLs were infected with rKSHV.219 and GFP-positive cells by FACS analysis (**A**) or amount of KSHV DNA by qPCR (**B**) were evaluated at the indicated time points. Experiment was performed with biological triplicates. (**C**) Immunofluorescence assay was performed to detect GFP-LANA (green) and Fc-MeCP2 (red). The nucleus was stained with DAPI. Scale bar = 5 µm. The average ratio between big and small foci are presented on the right, same as in Fig 2. (**D**) NIH 3T3 cells were transfected with GFP-LANA and wt MeCP2, T158M mutant, or del-MBD. Immunofluorescence assay was performed same as in C. Intensity profiles along the indicated arrows are presented on the right.

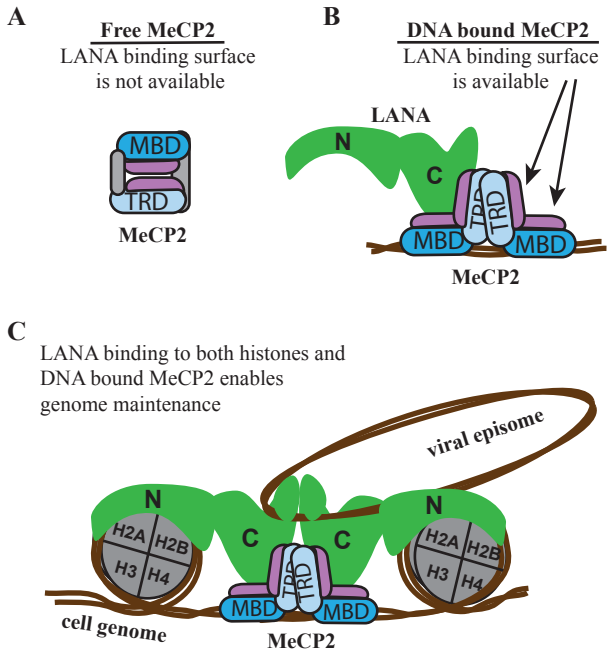

Figure 7. Schematic presentation of directional recruitment. (A) In its DNA free form, the MBD and TRD of MeCP2 are not available for LANA interaction. **(B)** Upon binding to methylated DNA LANA binding surface in MeCP2 becomes available for LANA binding. **(C)** LANA tethers the viral episomal genomes to cellular chromosomes by binding to histones via its N-terminal domain and to MeCP2 via its C-terminal domain. This unidirectional recruitment of LANA by MeCP2 is essential for viral genome maintenance during latency.